**Project title:** GaSTech

**Project ID:** 271511

**Funding scheme:** ERA-Net Cofund ACT (http://www.act-ccs.eu/calls/)

**Topic:** Research and innovation actions for $CO_2$ Capture and Storage (CCS)

**Starting date of project**: 1st of August, 2017

**Duration**: 36 months

| WP N° | Del. N° | Title | Contributors | Lead beneficiary | Nature | Dissemination level | Delivery date from Annex I | Actual delivery date |
|---|---|---|---|---|---|---|---|---|
| 3 | 3.6 | Performance assessment of GSOP process | Carlos Arnaiz del Pozo (UPM)<br><br>Ángel Jiménez Álvaro (UPM) | UPM | R | PU | 31/08/2020 | 14/09/2020 |

# Executive Summary

The scope originally envisaged for UPM has been extend to incorporate power plants integrating Gas Switching Combustion (GSC), given the low prospects for development of the Gas Switching Oxygen Production (GSOP) oxygen carrier within the time frame of the GaSTech project. Nonetheless, several power plants incorporating GSOP clusters have been evaluated. The baseline for GS technology evaluation assessment of power generation systems starting from a solid fuel and involving gasification units to obtain a suitable gaseous fuel to the cluster. Evaluation of natural gas fired power plants was left out of the scope from UPM in order not to conflict with parallel assessments from NTNU.

The key performance indicators, following the 4E analysis methodology (Energy, Environmental, Exergy and Economic*[1]) are defined in the first section of this report. UPM has developed a set of modelling blocks representative of several technologies appearing in Integrated Gasification Combined Cycles (IGCC) in the simulation tool Unisim Design R451. Alongside this, UPM has built an integrated model which can connect the transient GS reactor model to a stationary power plant simulation though a CAPE-OPEN unit operation. Also, a membrane reactor for $H_2$ production has been developed in Scilab 6.0.2. These reactor models are succinctly described in section 2. For a more detailed description of the power plant blocks (i.e. gasification, air separation etc.) the reader is referred to the appendixes of deliverable 3.4: Mass and energy balances and unit sizing of GSOP process.

Two sets of power plant simulations are presented. The "Introductory" power plants consist of base-load IGCC schemes employing a gas turbine (GT) with a performance analogous to an F-class machine. Flexibility with regard to the GT design is considered to account for particular implications of a GS(C) cluster or firing of $H_2/N_2$ mixtures and syngas. The "Advanced" power plants consist of an integration between GSC and the membrane assisted water-gas shift reactors (MAWGS) in an IGCC cycle which employs a more efficient, larger H-class GT. It was modelled with the assistance of Prof. Paolo Chiesa from Politecnica di Milano. The "Advanced" plants allow the possibility of producing $H_2$ from the MAWGS reactor as an energy vector at times when electricity prices are low. Both sets of plants have consistent IGCC benchmarks with and without CCS for reliable comparison between concepts. The analysis performed consist of an *ex ante* assessment, considering that several technological showstoppers such as high temperature valves and filters, as well as GT adaptations (for "Introductory" plants) have been realized by the time of 2$^{nd}$ generation CCS technology is deployed, around 2040.

The general conclusions for this study are that GS technology has a high potential to mitigate and reduce the energy penalty associated to $CO_2$ capture, in particular when combined with hot gas clean-up for syngas desulphurization, achieving relatively high levels of $CO_2$ capture rate and $CO_2$ avoidance. Nonetheless, the heat management strategies employed to maintain high average stage temperatures must be proven and de-risked. High temperature valves and filters must be available while oxygen carrier performance must be verified at large scale. Furthermore, substantial changes in turbomachinery components of the topping cycle must be undertaken for some of the concepts proposed, given the lower thermodynamic temperature of the cycle and changed flow pattern due to the GS cluster integration. The intrinsic advantage of load flexibility of gas switching clusters as opposed to interconnected fluidized beds allows power plants using this technology to operate

[1] Economic results are not provided in this report.

flexibly in order to balance variable renewable energy, producing alternative fuels or chemicals such as $H_2$, which can in turn aid to the decarbonize other sectors of the economy. This can be done by integrating the cluster with Pd-based membrane reactor, as shown in the "Advanced" power plant concepts described in this report.

From the "Introductory" power plants assessed in this study, the GSC IGCC concept with natural gas extra firing achieves around 2%-points higher efficiency than the Unabated IGCC benchmark with approximately 80% $CO_2$ avoidance. The Oxygen Production Pre-combustion (OPPC) IGCC plant replacing the ASU with a GSOP cluster has an energy penalty of only 1,5%-points with above 83% $CO_2$ avoidance. Regarding the "Advanced" $H_2$/power flexible IGCC plants, the pregasifier with HTW gasification concept reduces the energy penalty to only 1,3%-points, with almost complete carbon capture. The concept integrating a GE gasifier and partial water quench reaches similar electrical efficiencies as the Shell gasifier configuration, while operating the MAWGS with $N_2$ and steam sweep in the permeate side for power and $H_2$ production modes respectively, avoiding partially the costly $H_2$ compression to delivery pressures.

# 1. Key Performance Indicators

In this section, the performance metrics for the different power plant concepts are presented, attending to the 4E classification: Energy, Environmental, Exergy and Economic. The plant is defined with a boundary from which different material and energy streams are fed or produced, as depicted in Figure 1:

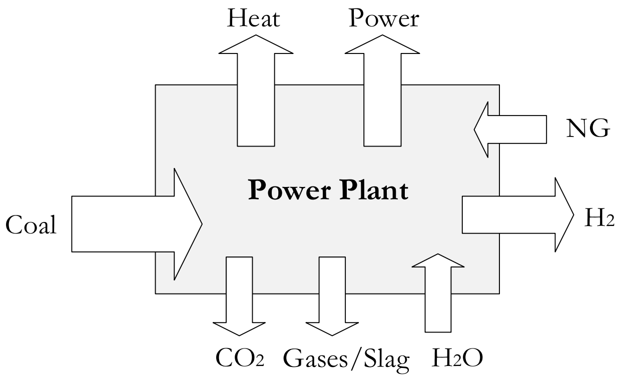


Figure 1 Simplified diagram of a power plant

## 1.1 Energy

The thermal efficiency of the power plants is defined on a low heating value basis (LHV) in this assessment. It provides a simple ratio between raw material investment (fuel) and useful output (electricity, hydrogen). The energy metrics are presented in Table 1, considering the possibility of $H_2$ co-production. In such scenario, the power plant may consume or produce some electrical power, therefore an equivalent efficiency is defined assuming a benchmark efficiency for the electrical power generation/consumption as if it were produced by this reference plant.

Table 1 Energy performance indicators

| | |
|---|---|
| Net Electrical Efficiency (%) | $\eta_t = \frac{\dot{W}_{net}}{\dot{m}_{coal} LHV_{coal}}$ |

| | |
|---|---|
| Hydrogen Efficiency (%) | $\eta_t^{H_2} = \dfrac{\dot{m}_{H_2} LHV_{H_2}}{\dot{m}_{coal} LHV_{coal}}$ |
| Hydrogen Equivalent Efficiency (%) | $\eta_{t,eq}^{H_2} = \dfrac{\dot{m}_{H_2} LHV_{H_2}}{\dot{m}_{coal} LHV_{coal} - \dfrac{\dot{W}_{net}}{\eta_{t,ref}}}$ |

The net electricity output is a simulation results obtained from subtracting the auxiliary consumption of the different process units in the plant from the gross power output delivered by the topping and bottoming cycles.

## 1.2 Environmental

Environmental assessment is focused solely in $CO_2$ emissions, given the fact the IGCC technologies offer a substantial reduction in sulphur and particulate emissions relative to pulverized coal (PC) boilers. The use of chemical looping also avoids NOx formation in several of the concepts presented due to the flameless combustion taking place in the reactors of the GS cluster. Although the power plant capture rate is a fast way to evaluate the $CO_2$ mitigation capability of a power plant, it falls short in the sense that the implementation of CCS will imply a bigger amount of fuel consumption (and thus $CO_2$ generation) per unit of electricity produced, relative to a plant without CCS. This is represented in Figure 2:

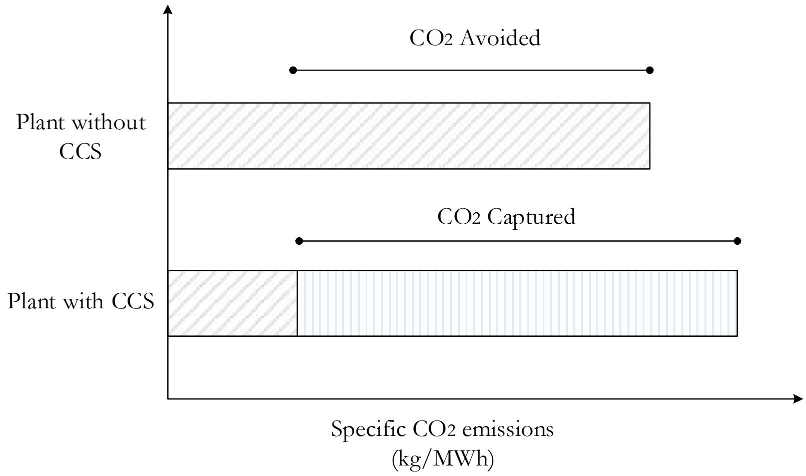


Figure 2 $CO_2$ avoidance vs. $CO_2$ capture

The capture rate is directly accessible from the $CO_2$ streams leaving the plant boundary from the simulation model. The $CO_2$ avoidance is calculated following the equations provided in Table 2, using the specific emissions (determined as the $CO_2$ emitted divided by the net power output).

Table 2 Environmental performance indicators

| | |
|---|---|
| $CO_2$ Capture rate (%) | $C_{CO_2} = \dfrac{\dot{m}_{CO_2,capt.}}{\dot{m}_{CO_2,em.} + \dot{m}_{CO_2,capt.}}$ |

| | |
|---|---|
| Specific Emissions ($kgCO_2/MWh$) | $E_{CO_2} = \frac{\dot{m}_{CO_2,em.}}{\dot{W}_{net}}$ |
| $CO_2$ Avoidance (%) | $A_{co_2} = \frac{E_{CO_2,Ref} - E_{CO_2,CCS}}{E_{CO_2 Ref}}$ |
| SPECCA ($MJ/kgCO_2$) | $SPECCA = 3600 \frac{\frac{1}{\eta_{t,CCS}} - \frac{1}{\eta_{t,Ref}}}{E_{CO_2,Ref} - E_{CO_2,CCS}}$ |

The Specific Primary Energy Consumption of $CO_2$ Avoided (SPECCA) accounts for the amount of heating value from the original fuel invested in achieving the $CO_2$ capture, relative to a power plant without CCS. Its value may be negative in the case the efficiency of the plant with CCS is higher than the reference unabated plant.

## 1.3 Exergy

Exergy is a thermodynamic function of state which allows to determine a rational efficiency of the power plant taking into account second law limitations. The definition of the exergy efficiency depends on the items that are considered as a useful effect, as shown in Table 3. The process unit irreversible losses $\dot{I}_j$ are determined with the exergy balance, which enables a better understanding of the novel configurations. Such thermodynamic mapping was carried out to all of the "Introductory" power plants. An analysis of the main input and output exergy streams from the "Advanced" plants was also performed.

Table 3 Exergy performance indicators

| | |
|---|---|
| Exergy Efficiency (%) | $\xi = \frac{\dot{W}_{net} + \dot{E}_{H_2}}{\dot{E}_{coal}} = 1 - \frac{\sum \dot{I}_j + \sum \dot{E}_{out}}{\dot{E}_{coal}}$ |
| Exergy Efficiency considering other useful outputs (%) | $\xi' = \frac{\dot{W}_{net} + \dot{E}_{H_2} + \dot{E}_{CO_2} + \dot{E}_{Steam}}{\dot{E}_{coal}}$ |

The exergy of the fuel, $\dot{E}_{coal}$ is estimated using a correlation [1].

## 1.4 Economic

The economic metrics are not reflected in this report. The reader is referred to deliverable 4.1: Economic assessment of two process concepts, for more information regarding the economic performance of the plants presented in this report.

# 2 Reactor Models

In this section, a brief description of the models developed by UPM is provided. The GSC model was created to accomplish an integrated simulation of the cluster and power plant in order to save time and reduce interfaces of information exchange. The description of the technological blocks of the power plants can be found in detail in deliverable 3.4, carried out by the same authors of the present report.

## 2.2 GSC

The model solved in Scilab is analogous to the one described in deliverable 3.1 carried out by NTNU and SINTEF in Matlab [2]. It consists of performing mass and energy balances to a dynamic continuous stirred tank reactor (CSTR), which represents a fluidized bed. The model assumes therefore complete mixing of inlet streams and additionally, ideal gas behaviour and full fuel conversion. The equations solved by the model are summarized in Table 4:

Table 4 GS reactor model equations

| | |
|---|---|
| Mass Balance | $\frac{dn_k}{dt} = F_{in}y_{in,k} + F_{out}y_{out,k} + \sum_{r=1}^{R} \upsilon_{r,k}\xi_r$ |
| Energy Balance | $\frac{dT}{dt} = \frac{-F_{in}\sum_k y_{in,k}\int_{T_{in}}^{T} c_{p,k}dT + \sum_{r=1}^{R}\xi_r(-\Delta H_{r,T})}{\sum_k n_k\, c_{p,k}}$ |
| Outlet flow calculation | $F_{out} = F_{in} + \sum_{R}^{k\in gases} \upsilon_{k,r}\xi_r + \frac{PV_{gas}}{RT^2}\dot{T}$ |

Kinetic expressions are identical as in the Matlab model, while similar heat management strategies have been coded in the Scilab version for integration in the power plant (except steam purging):

1. $N_2$ recycle
2. $O_2$ slip
3. Delayed switch

Besides the integration with the stationary power plant simulation, minor modifications relative to the model in Matlab have been performed:

- The Scilab model evaluates the properties of each component at every instantaneous temperature across the cycle. This predicts the enthalpy of reaction more accurately, which has resulted in a temperature rise during the reduction stage of the NiO/Ni cycle, for specific reactor conditions.
- The Scilab model has a data processing code of the instantaneous stage outlet of any cluster configuration: allowing to define more than 1 reactor operating in reduction, i.e. 2 in reduction and 5 in oxidation. Essentially, this reduces the output fluctuations of temperature and flow rate, since a better phasing between each reactor in the cluster is reached.

- Two parameters for the degree of mixing between outlet streams of a reactor are defined. One for $CO_2$ recovery in the reduction stream and another one for the $N_2$ slip from the oxidation outlet.
- The delayed switch time is optimized to maximize $CO_2$ recovery in each simulation run.

## 2.3 MAWGS

The MAWGS model integrated with the GSC and power cycle of the "Advanced" plants constitutes a relevant building block of the latest studies performed by UPM, and therefore a brief description of it is presented here. The 1-D code in Scilab solves the mass and energy balance across a plug flow reactor (PFR) of predefined length and tube diameter. The retentate is the shifted syngas, while the permeate side is $H_2$ which has diffused across the reactor length. The reactor can be fed with a sweep gas ($N_2$ or steam) in the permeate side and flow countercurrently with respect to the reacting stream in order to maximize $H_2$ extraction at high pressure or, alternatively, operate at low permeate pressure with no sweep gas, to enable sufficient diffusion driving force. The balance and constitutive equations (kinetic and diffusion) are provided in Table 5 for permeate and retentate streams:

Table 5 MAWGS reactor model equations

| | |
|---|---|
| Mass Balance | $\frac{\partial f_{k,R}}{\partial z} = r_{k,R}\rho_s w_c(1-\varepsilon)\frac{\pi d_t^2}{4} - \pi d_t \phi''_{k,R}$ |
| | $\frac{\partial f_{k,P}}{\partial z} = -\pi d_t \phi''_{k,R}$ |
| Energy Balance | $\frac{\partial T_R}{\partial z} = \frac{-\sum h_{k,R}\frac{\partial f_{k,R}}{\partial z} + U\pi d_t(T_P - T_R)}{\sum f_{k,R}c_{pk,R}}$ |
| | $\frac{\partial T_P}{\partial z} = \frac{-\sum h_{k,P}\frac{\partial f_{k,P}}{\partial z} + U\pi d_t(T_P - T_R)}{\sum f_{k,P}c_{pk,P}}$ |
| Kinetic Rate [3] | $r_k = \nu_k k P_{CO}^a P_{CO2}^b P_{H2}^c P_{H2O}^d \left(1 - \frac{P_{H_2}P_{CO_2}}{K_{eq,WGS}P_{CO}P_{H_2O}}\right)$ <br> $lnK_{eq,WGS} = \frac{4577{,}8}{T} - 4{,}33$ |
| Diffusion Rate [4] | $\phi''_k = \frac{P_0}{t_m} e^{\left(\frac{-E_a}{RT}\right)}\left(P_{k,R}^{0.74} - P_{k,P}^{0.74}\right)$ |

Numerically, solving the MAWGS model in countercurrent operation is more complex because the boundary condition for the differential equation must be firstly assumed (temperature and $H_2$ flow rate of the permeate at length z=0) and then iteratively converged. A reactor profile for temperature, $H_2$ partial pressure is given in Figure 3 (above) while a retentate composition profile and % permeate flow are shown in Figure 3 (below).

Given the low price of membrane surface, in the current simulations the MAWGS reactor is oversized for power production mode (with syngas by-pass directly to the GSC), while $H_2$ production is maximized when switching from operating mode. The models presented in this report employ 6000 membrane tubes with 10m height and 0.05m diameter, which correspond to approximately 5% of the specific investment cost of the plant. Extra surface area of membrane is also a positive feature to enhance plant availability and carry out reactor maintenance and replacement with minimum turndown of the plant.

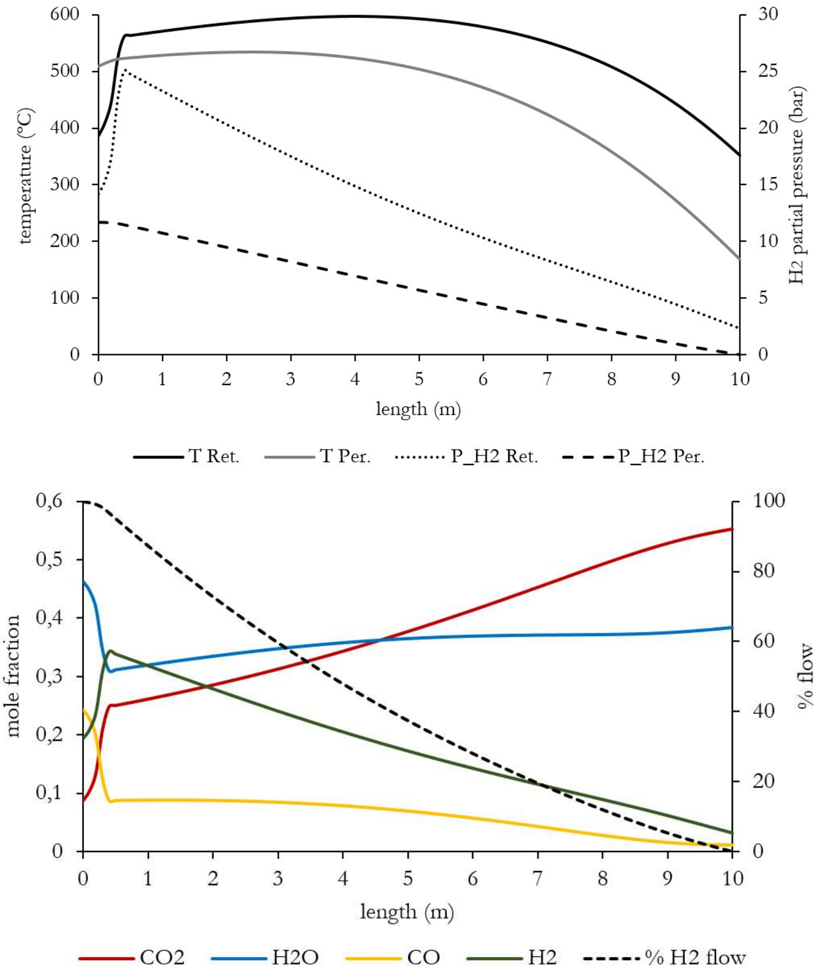


Figure 3 MAWGS reactor profiles

# 3 Power Plant Concepts

In this section a block flow diagram of the “Introductory” plants using F-class GT performance is provided. The F-class machines was simulated and calibrated in Unisim for a reference natural gas fired case [5], while nominal component efficiencies and operational values were employed in the models. A short, qualitative description of the plant main features is given. Detailed description of the models can be found in deliverable 3.4 and will not be repeated here. On the other hand, the process diagrams for the “Advanced” power plants with H-class turbines adjusted the coal input to meet the GT size constraints, and the pressure ratio was modified accordingly to flow rate variations in each model. Unless stated otherwise, the oxygen carrier employed in the GSC is Ni/NiO, which shows the most promising properties for fluidization at high temperatures.

## 3.1 "Introductory" Power Plants

As mentioned earlier, these plants assume a fixed coal flow rate and that appropiate modifications to the turbomachinery components can be realized to cope with the changed flow pattern of syngas/$H_2$ fuel and integration of GS clusters. The steam cycle, applied to many of the concepts, consists of a three pressure level reheat configuration as described in [6].

### Unabated IGCC

Power plant depicted in Figure 4 designed according to [5, 7]. Full nitrogen integration under the assumption that the compressor can cope with a comparatively reduced air flow results in somewhat higher efficiencies.

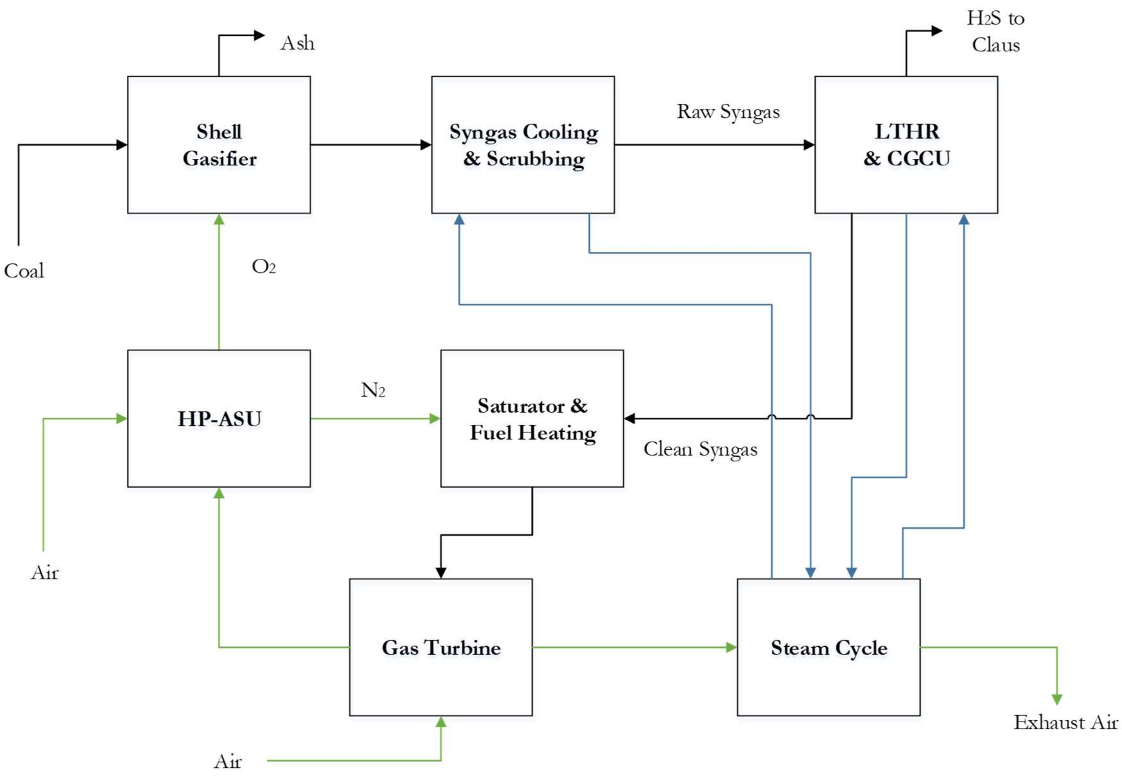


Figure 4 Unabated IGCC process diagram

### Pre-combustion $CO_2$ capture IGCC

Power plant designed according to [5, 7] and represented in Figure 5. Detailed model description can be found in [8, 9]. Selexol absorption was modelled using thermodynamic data from [10].

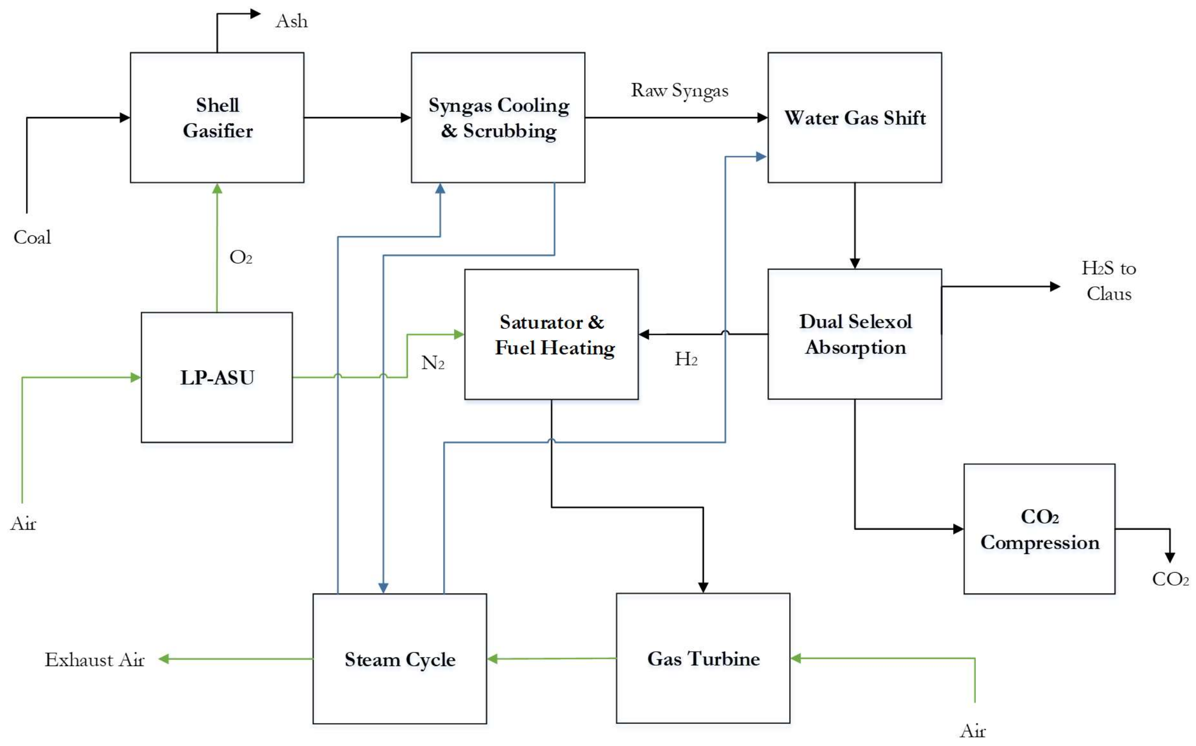


Figure 5 Pre-combustion $CO_2$ capture IGCC process diagram

## Standalone GSC IGCC

Integration of GSC in IGCC power plant, using $N_2$ recycle to the GT compressor to maximize oxidation outlet temperature and $CO_2$ capture rate, similarly to [2, 11] and shown in Figure 6:

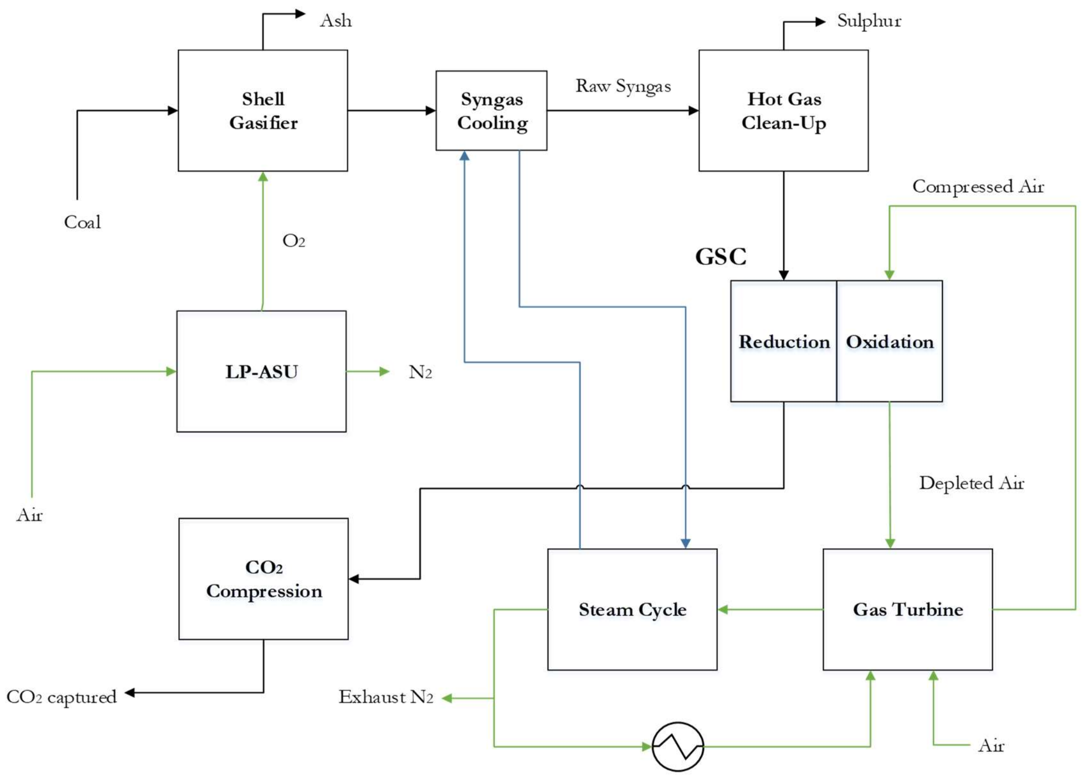


Figure 6 Standalone GSC IGCC power plant

## GSC with NG Extra Firing IGCC

As depicted in Figure 7, extra firing chamber with NG is added to increase turbine inlet temperature (TIT) to F-class GT values [11].

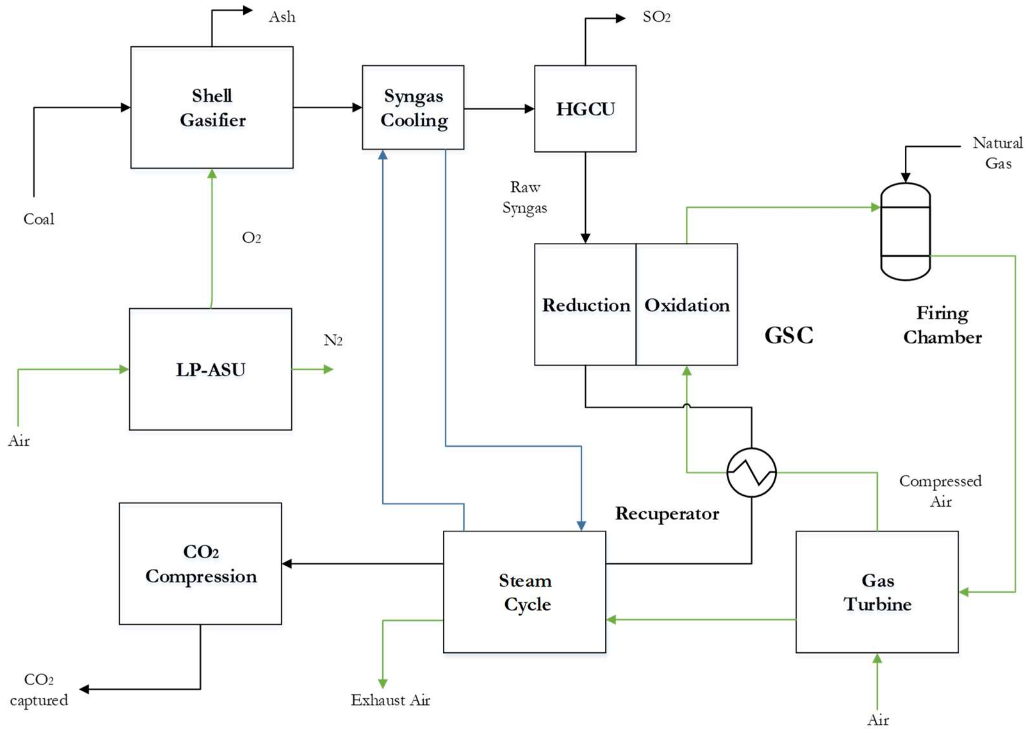


Figure 7 GSC with Extra Firing IGCC process diagram

## Integrated gasification GSC-HAT

The GSC cluster operating with $N_2$ recycle is integrated in a slurry fed gasifier with partial water quench cooling and a humid air turbine power cycle (HAT) [8], as shown in Figure 8.

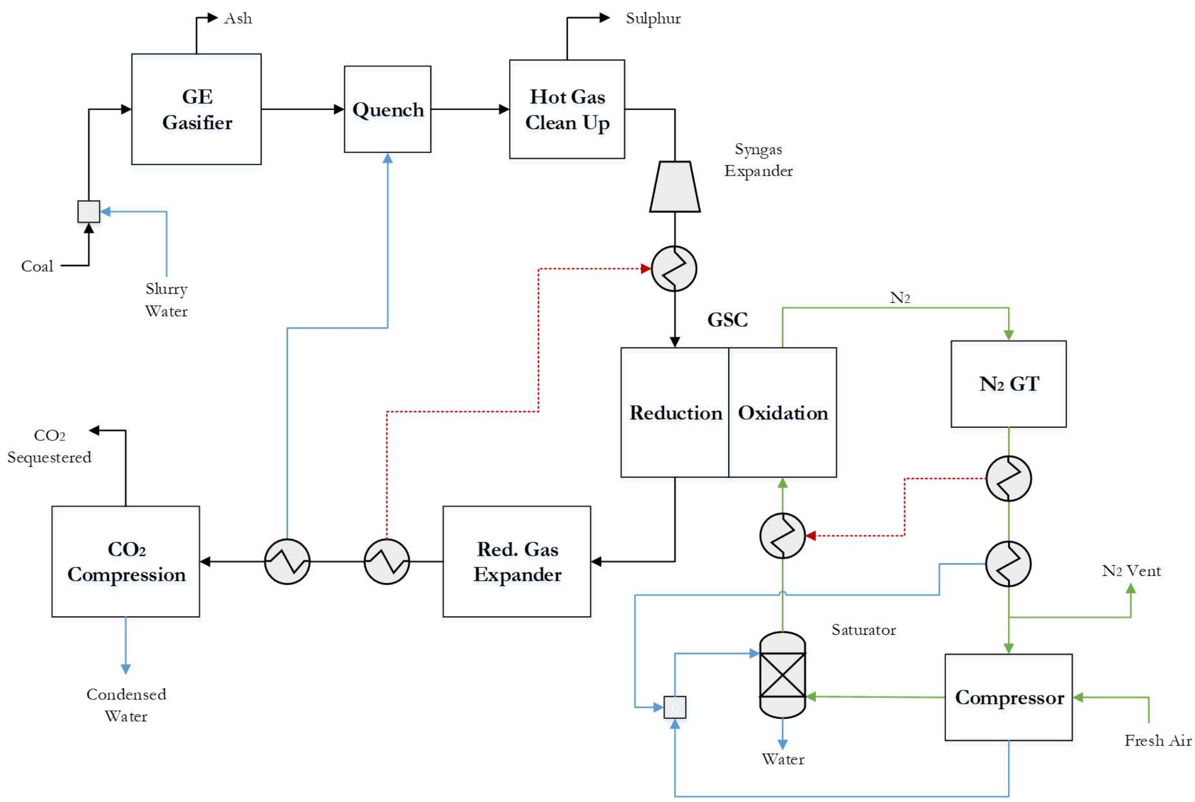


Figure 8 Integrated gasification GSC-HAT process diagram

## Oxygen Production Pre-combustion IGCC[2]

Integration of a GSOP cluster in a fluidized bed Winkler gasifier, extensively studied in [12]. The case presented in this report and shown in Figure 9 assumes no $H_2$ dilution for extra firing is required. The gasification fixed carbon conversion was set to 97% according to [13]. The GSOP operating temperature is 900ºC, adjusting the kinetic expression for $O_2$ production from [14].

[2] A correction made to the OPPC model simulation indicated a higher efficiency than the one reported in deliverable 3.4. The value presented in the present report is valid and should be considered for future evaluations of the concept.

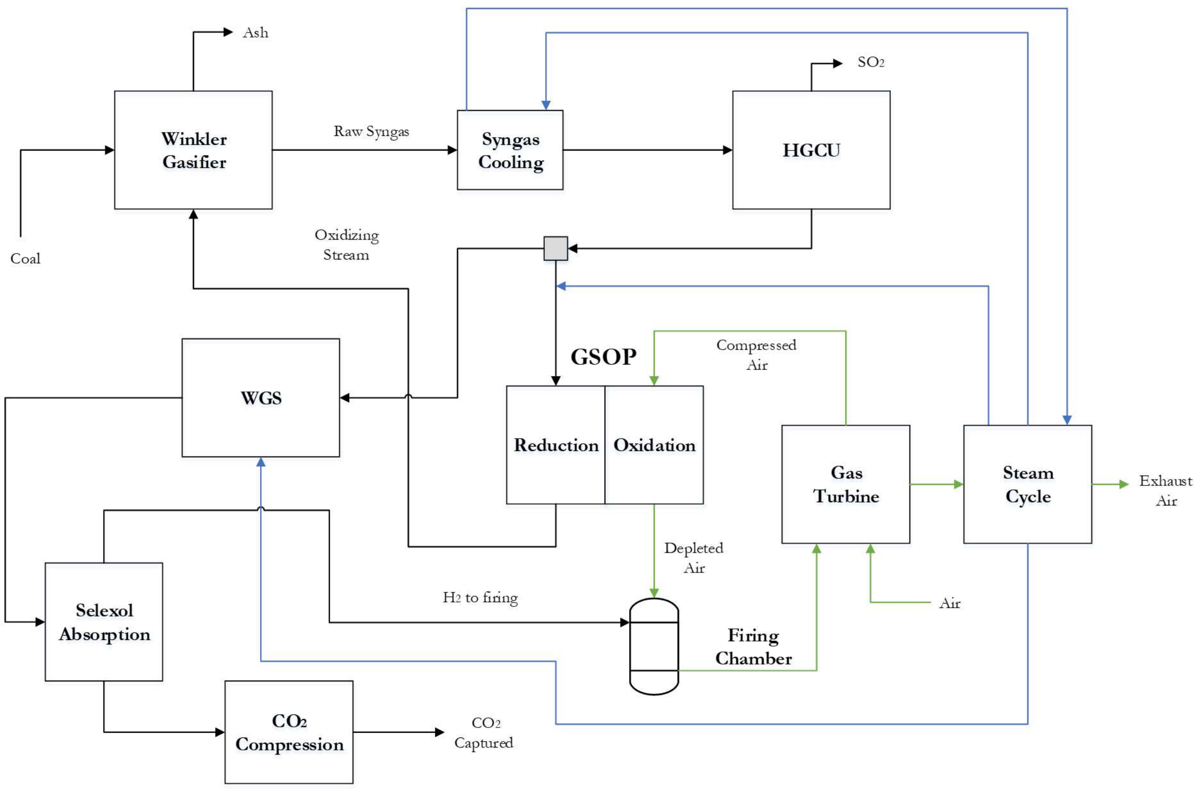


Figure 9 Oxygen Production Pre-combustion IGCC process diagram

## Composite GSC-GSOP IGCC

As depicted in Figure 10, it consists of an integration of GSOP, GSC and Winkler gasifier, eliminating the energy penalty of ASU and obtaining a pressurized $CO_2$ stream, extensively studied in [8]. High level of mixing reduces capture, but efficiency results somewhat higher than in [14]. For this case, a slightly lower carbon conversion (95.5%) of the Winkler gasifier is assumed (consistently to the previous reference) and the GSOP operating temperature is 700ºC (the kinetic expression is adjusted). Oxygen carrier in GSC is Ilmenite, which results in a higher mixing degree, for the same average oxidation temperature, relative to Nickel.

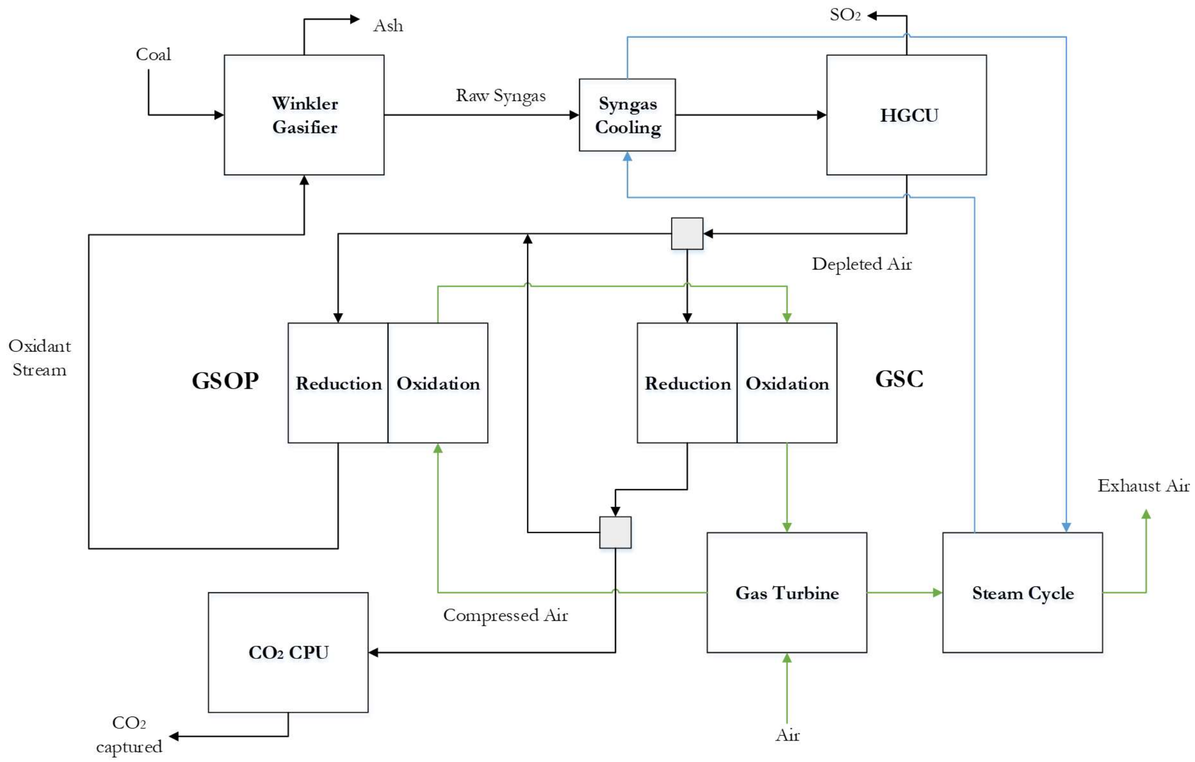


Figure 10 Composite: GSOP-GSC IGCC process diagram

A comparison between the different "Introductory" concepts highlighting advantages and drawbacks as well as key technological gaps is given in Table 6:

Table 6 Assessment of "Introductory" power plants

| Power Plant Type | Benchmarks | | GSC | | | GSOP | |
|---|---|---|---|---|---|---|---|
| **Concept/ KPI** | ***Unabated IGCC*** | ***Pre-combustion $CO_2$ capture IGCC*** | ***Standalone GSC IGCC*** | ***GSC with Extra Firing IGCC*** | ***Integrated Gasification GSC-HAT*** | ***Oxygen Production Pre-combustion (OPPC) IGCC*** | ***Composite: GSOP-GSC IGCC*** |
| **Key Advantages** | Inherently more efficient than PC boilers | Effective removal of $CO_2$ before fuel combustion | Inherent $CO_2$ capture. Low energy penalty and avoidance of NOx due to flameless combustion | Temperature can be raised to actual GT technology leading to higher efficiencies. Costly gasification island can be downsized relative to the power cycle | Possibility to operate flexibly decoupling reduction & oxidation sections to balance VRE. Reduction section can be downsized with reduced cost prospects. | Ability to raise TIT through carbon free fuel in an extra firing stage, and consequently thermodynamic efficiency | Inherent carbon capture and avoidance of ASU, which results in high efficiency |
| **Key Drawbacks** | No $CO_2$ capture. High capital expenditure | Large energy penalty and associated cost | Limited reactor temperature reduces cycle thermodynamic efficiency | Carbonaceous emissions arise from extra firing of NG. | Low reactor temperature results in low efficiency. Quench design for syngas cooling and HAT cycle have lower efficiency relative to an integrated CC. | Lower capture rate due to methane slip. Lower performance of the Selexol plant due to lower operating pressures. | Complex integration of two GS clusters for an inflexible scheme. Low attainable temperature in GSC limits thermodynamic efficiency. High level of mixing in the 2 clusters lowers capture rate |
| **Technology Gaps** | GT adapted to syngas fuel | GT must be adapted to use $H_2/N_2$ mixture as fuel | HGCU must be demonstrated. High temperature valves and filters and oxygen carrier material development. | High temperature valves and filters and oxygen carrier material development. Heat management to ensure low mixing must be demonstrated at large scale. HGCU must be demonstrated | HAT cycle is not yet commercial. Coupling the reduction section turbomachinery can be challenging HGCU must be demonstrated. High temperature valves and filters and oxygen carrier material development. | Oxygen carrier is at a very early stage of development and must be demonstrated at lab scale. $H_2$ firing might require dillution and diffusive flame combustion to limit NOx. Gasification technology not implemented in large scale IGCC. HGCU must be demonstrated. | High temperature valves and filters, oxygen carrier material development for GSOP. Gasification technology not implemented in large scale IGCC. HGCU must be demonstrated. |

## 3.2 "Advanced" Power Plants

"Advanced" power plant models consist of IGCC plants which incorporate modern H-class GT machines, capable of reaching higher combustion temperatures than F-class machines due to an improved blade cooling technology. The main parameters of the H-class machines for natural gas firing are summarized in Table 7.

Table 7 H-class machine specifications

| Item | Value | Units |
|---|---|---|
| COT | 1648 | °C |
| TIT | 1550 | °C |
| TOT | 641 | °C |
| Simple cycle efficiency | 43,0 | % |
| Pressure ratio | 23,6 | - |
| Rated Power | 520 | MW |

The H-class GT was modelled using the GS code from Politecnica di Milano by Paolo Chiesa. Iterative runs were established in order to reach the coal input which yielded the same air and fuel flow rates between the GS code and the stationary model in Unisim. All designs were evaluated for the same reference COT.

### Unabated IGCC

The same power plant concept as applied to the corresponding introductory plant, but incorporating hot gas clean up with adsorbents, following a similar modelling procedure as in [15] for this process unit. Syngas fuel dilution with $N_2$ from ASU and steam from the HP stage outlet of the steam turbine was performed to limit stoichiometric flame temperature at 2200K, thus avoiding unacceptable NOx formation. The steam cycle has some minor differences with respect to the "Introductory" plants model. Namely, the HP evaporator is a once through heater (avoids the HP stage drum and recirculation loop) and the maximum steam temperature was 600ºC (making use of the higher turbine outlet temperature TOT of the H-class turbine). Finally, the condensing steam pressure was set to 40 mbar, resulting in a condensing steam temperature of approximately 28ºC.

### Pre-combustion $CO_2$ Capture IGCC

The process model for the "Advanced" pre-combustion plant is very similar to the one provided in the "Introductory" power plant subsection, except that as in the Unabated IGCC case, HGCU technology is employed to remove sulphur components and other contaminants from the syngas. The advantages of HGCU in this model are to some extent curtailed because cooling of the syngas is still required to absorb $CO_2$ after water gas shift (WGS). However, since $H_2S$ has already been removed, the Selexol plant is considerably simpler, reducing significantly the auxiliary duty of solvent pumping. Furthermore, due to the high temperature after HGCU, part of the steam addition required prior to the high temperature shift (HTS), is provided as hot IP water, quenching the stream to appropiate inlet temperature to the shift reactor. The $H_2$-rich fuel after absorption is mixed with $N_2$ from the ASU is saturated with water to limit NOx emissions upon combustion with air. The process diagrams of the two "Advanced" benchmark schemes are provided in

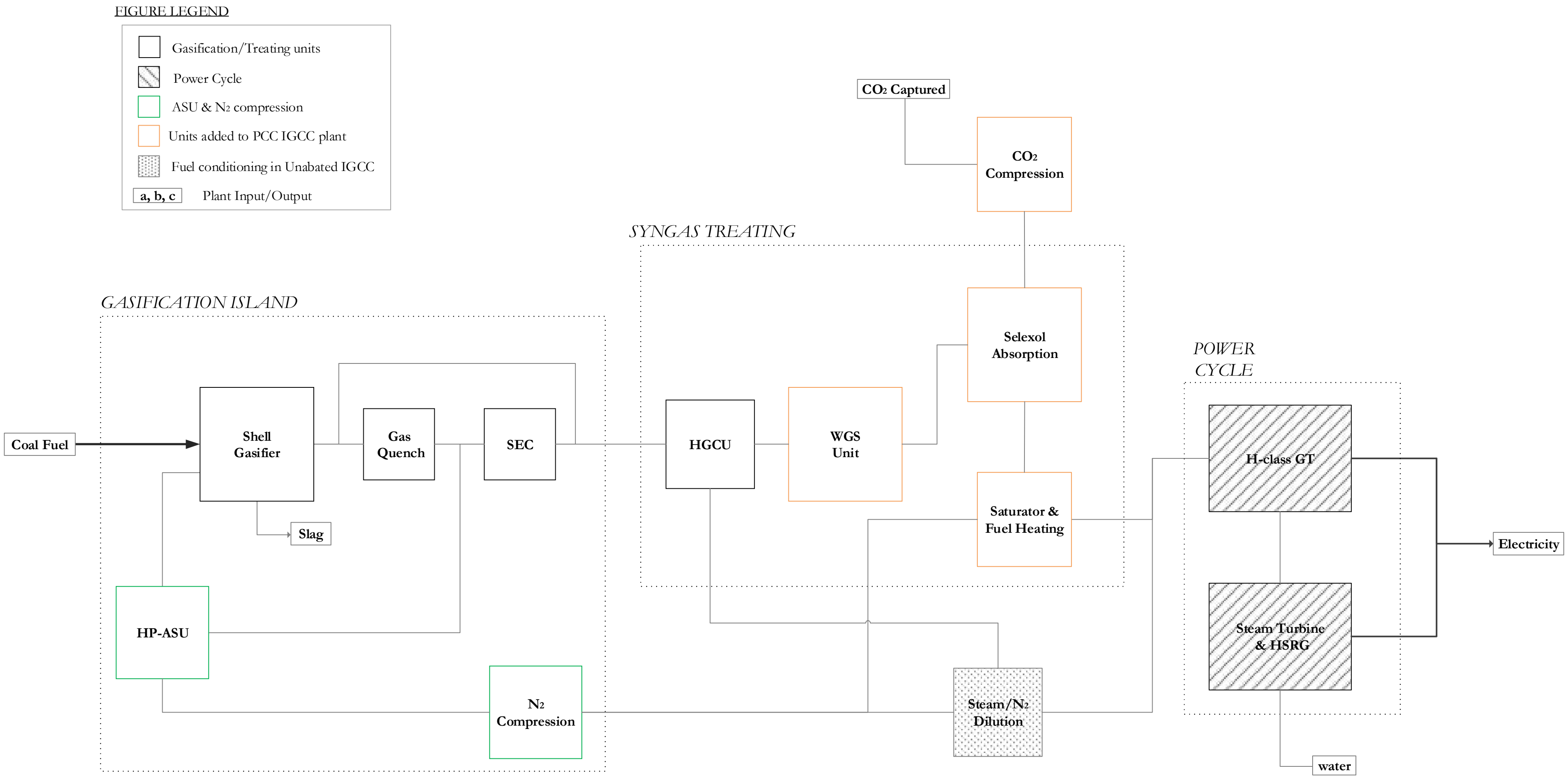


Figure 11 "Advanced" Unabated and Pre-combustion $CO_2$ capture process diagram

## GSC-MAWGS IGCC power plants

The GSC-MAWGS IGCC power plants operate under the concept depicted in Figure 12 . At low electricity prices, $H_2$ generation is favoured. In power production mode, the membrane reactors are operated such that only sufficient $H_2$ is produced to reach the COT value of the H-class GT after the GSC oxidation outlet. A more detailed depiction of the different GSC-MAWGS IGCC power plant configurations with different gasification systems is given in Figure 13:

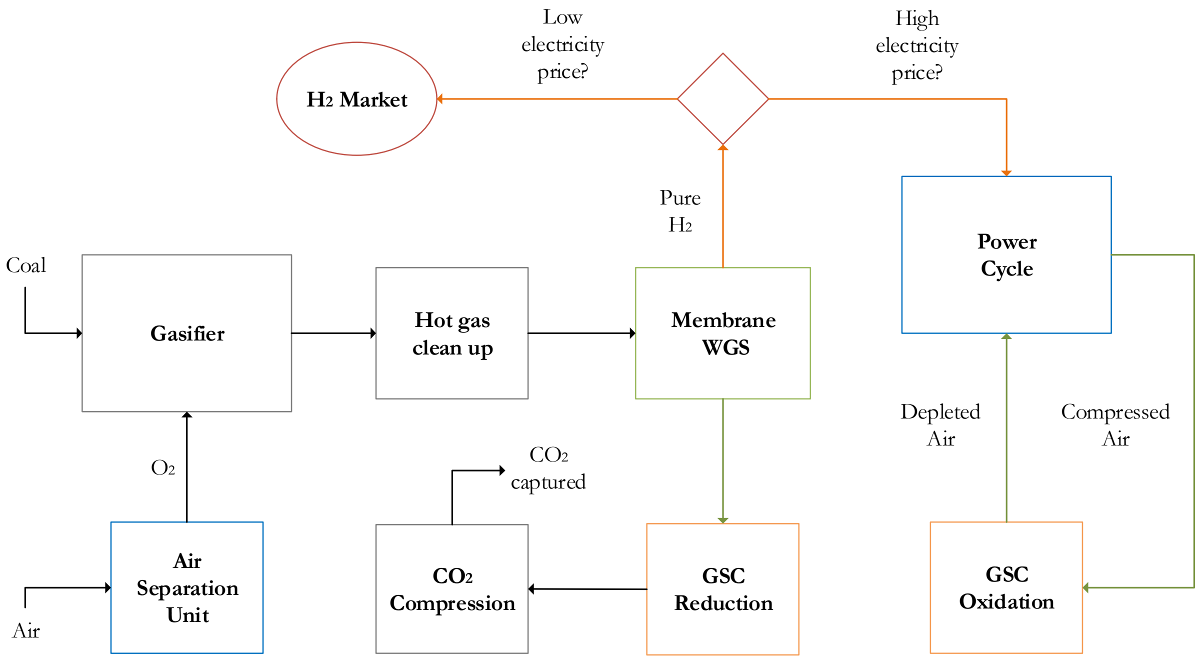


Figure 12 GSC-MAWGS IGCC power plant concept [16]

All of the plants presented in this section operate the GSC cluster with the $O_2$ slip heat management strategy to maintain high average oxidation outlet temperature as well as low stream mixing (with longer cycles). This reactor operation should be further demonstrated. Alternative process line-up which do not require to maintain a high GSC average temperature may be desirable, if sufficient $H_2$ in the MAWGS can be produced to reach COT values in the extra firing chamber. This will result in a slight efficiency penalization due to more fuel conversion in the MAWGS and associated losses.

### *GSC-MAWGS IGCC with Shell gasification*

The GSC-MAWGS concept is integrated with the Shell gasification system. The high cold gas efficiency (CGE) allows to reach a high heating value in the form of $H_2$ product and electrical efficiency in both modes of operation. However, $N_2$ from the ASU is not sufficient to reach COT values of the GT, and $H_2$ fuel compressor is necessary. A reduction gases recuperator with the fuel stream routed to the GSC reinjects part of the heating value of the fuel to the topping cycle. In $H_2$ mode, system's flexibility is a challenge as a high amount of steam is generated in the syngas effluent coolers (SECs). Operation of the GT at very low partial load (10% GT) may cause substantial changes in syngas expander, $CO_2$ compressor and recuperator operating points. A small air turbine coupled with the GSC and a smaller heat recovery network (relative to the HSRG) is proposed as an alternative.

### *GSC-MAWHS IGCC with Pregasifier and HTW gasification*

A slurry pregasification with the heat contained in the reduction gases ex. GSC and the use of a Winkler gasifier results in high CGE efficiency with very low ASU consumption, which ultimately translates into very high electrical and hydrogen efficiencies. Variations in GSC operating points when switching from $H_2$ to power production may cause changes in performance in the pregasifier unit, with a convoluted effect in the whole process. A small GT operation in $H_2$ mode is proposed to mitigate this effect to an extent. This concept attains the highest electrical and $H_2$ efficiencies, although the assumptions made for pregasification and conversion of the slurry in the preheating unit may be optimistic.

### *GSC-MAWGS IGCC with GE gasification*

The use of a slurry fed entrained flow gasifier allows to raise the operating pressure to up to 80 bar, maximizing the driving force across the membrane and thereby extracting more $H_2$ comparatively to the earlier cases, which compensates the slight loss in CGE relative to the previous concepts. Syngas cooling is performed initially with a partial water quench followed by a syngas effluent cooler. Again steam production from syngas cooling can present a problem in $H_2$ operating mode (where the steam cycle is not entirely operative) and it is assumed the IP steam resultant after HP expansion is exported outside battery limits. The high syngas pressure allows the use of a small fraction of the ASU nitrogen to operate the MAWGS countercurrently and deliver diluted fuel stream for extra firing without the need of dedicated $H_2$ fuel compressors (intercooled $N_2$ compressor are used previously to the sweep feeding). In $H_2$ production mode, besides the option of operating the permeate side at low pressure without sweep gas and exporting residual IP steam from the plant, this steam (generated in the heat recovery units and after HP expansion) can be re-used again in the process as sweep gas to extract $H_2$, avoiding entirely the initial $H_2$ compression stages. Only LP steam is therefore exported from the plant in this scenario.

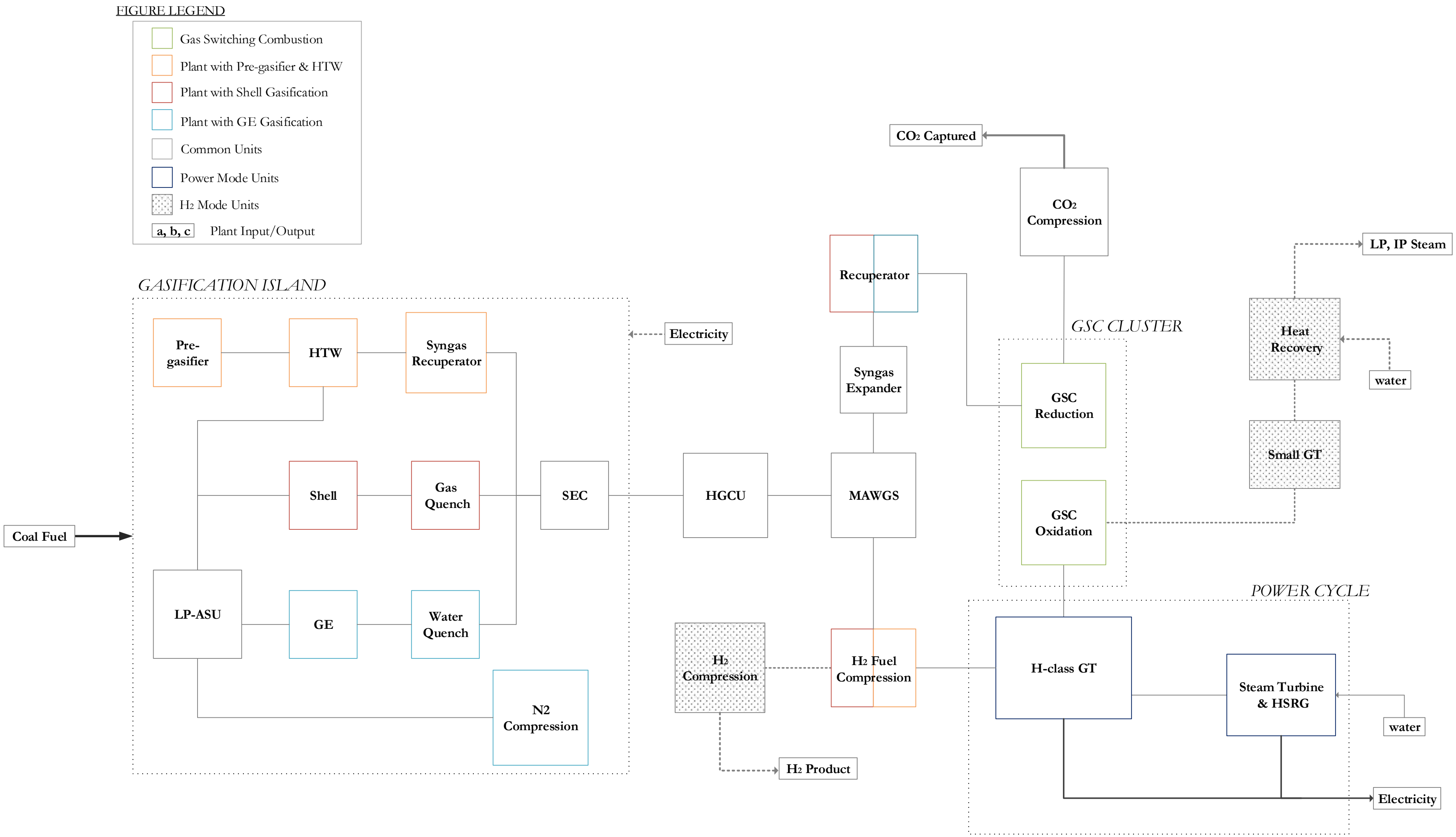


Figure 13 GSC-MAWGS IGCC power plant configurations

# 4 Summary of Results

Results are shown in two subsections, following the same power plant categorization of the previous sections and attending to the methodology described in section 1.

## 4.2 "Introductory" Power Plants

The process performance indicators defined in section 1 are presented in Table 8 for the "Introductory" power plants. The Unabated IGCC case was used as reference plant without CCS.

The main conclusions drawn is that the energy penalty incurred upon by conventional pre-combustion capture technology (which amounts to approximately 9%-points) can be clearly reduced by GSC and GSOP concepts provided the assumed reactor performance is reached and technological showstoppers are overcome. Namely, the standalone GSC IGCC plant with HGCU reduced the energy penalty by 5,6 %-points. The OPPC IGCC concept shows substantially higher performance at the cost of around 8%-points $CO_2$ avoidance reduction, and it employs a gasification system which has not been commercialized yet at large scale IGCC and material development of the GSOP carrier is required. However, it overcomes the intrinsic efficiency penalty imposed by the temperature limitations of the GSC concept. GSC with NG extra firing and reduction gases recuperator delivers very appealing efficiencies with a $CO_2$ avoidance loss of approximately 10%-points. The $O_2$ slip strategy for GSC operation must be proven to maintain high GSC temperature and limit as much as possible the degree of extra firing required. Alternatively, $H_2$ firing can potentially be used to maintain high efficiencies with elevated capture rates. Finally, the Integrated Gasification GSC-HAT process is a concept which can potentially operate flexibly upon electricity demand with a better performance than pre-combustion capture and almost complete $CO_2$ avoidance, although the power cycle has not been commercialized yet. The COMPOSITE process, although it promises high efficiencies, requires a complex integration between two GS clusters, and was ultimately neglected for future evaluation given a previous economic assessment carried out for packed bed GSOP-GSC integration, which revealed a low attractiveness of replacing the ASU with the GSOP [17].

## 4.3 "Advanced" Power Plants

The process performance metrics defined in section 1 are presented in Table 9 for the "Advanced" power plants. For the $H_2$ production mode, the case with an additional small air turbine is shown. This avoids the large changes in operating point for syngas expanders, recuperators, pregasification and $CO_2$ compression, outweighing the small extra investment cost. In the plant with Shell and GE gasification, it is assumed that only the first stage of the steam turbine operates at part-load, while the remaining steam flows (IP and LP) generated from the heat recovery units are exported from the plant. Furthermore, the GE gasification case avoids the initial stages of $H_2$ compression both in power (where $N_2$ from the ASU is used) and $H_2$ production modes (with IP steam sweep). The Unabated IGCC case was used as reference plant without CCS. The pregasifier with HTW gasification plant does not require the use of the HP stage steam turbine, given the fact that most of the syngas cooling is performed in the recuperator.

The benchmark plant results convey that the benefits of HGCU are to some extent mitigated: in the Unabated IGCC model, dilution with $N_2$ at a lower temperature and primarily steam extraction from the bottoming cycle in order to limit NOx emissions decrease the attainable efficiency. In the pre-combustion model, although the Selexol plant is simpler and steam addition is less inefficient (due to direct partial water quench to meet the required steam/CO ratio), the syngas must be cooled down to ambient temperature for $CO_2$ removal through absorption. The GSC-MAWGS IGCC concepts employing Shell and GE gasification attain similar efficiencies (a reduction in the energy penalty of more than 5%-points), yet the latter achieves a higher $H_2$ efficiency because of the larger driving force across the membrane caused by the higher operating pressure of the GE gasifier. The syngas pressure is higher due to the slurry feeding mechanism as opposed to pneumatic loading via lock hoppers in the Shell gasifier. The pre-gasification and HTW plant reveals very high efficiencies, but the carbon conversion assumed in the pregasifier unit and low $O_2$ demand of the HTW gasifier are elements of high uncertainty. Furthermore, the shifting from power to $H_2$ mode will cause changes in the GSC reduction outlet temperature that will affect the coal pregasification exchanger and therefore the overall performance of the gasification island. Detailed economic assessments taking into account the flexibility potential for $H_2$ and electricity production will balance the advantages and drawbacks that each of the concepts presented. Other heat recovery methodologies should be evaluated to make effective use of the excess steam generated in $H_2$ mode, for instance, maximization of LP steam production, IP bypass to the LP level and part load operation of the LP stage turbine could be a possibility.

Table 8 "Introductory" power plant results

| ***Power Plant Type*** | ***Benchmarks*** | | ***GSC*** | | | ***GSOP*** | |
|---|---|---|---|---|---|---|---|
| *Concept/ KPI* | **Unabated IGCC** | **Pre-combustion $CO_2$ capture IGCC** | **Standalone GSC IGCC** | **GSC with Extra Firing IGCC** | **Integrated Gasification GSC-HAT** | **Oxygen Production Pre-combustion (OPPC) IGCC** | **Composite: GSOP-GSC IGCC** |
| ***Energy*** | | | | | | | |
| $\eta_t^w$ *(%)* | 47,6 | 37,8 | 43,4 | 49,5 | 41,6 | 46,3 | 46,3 |
| ***Environmental*** | | | | | | | |
| $E_{CO_2}$ *(kgCO₂/MWh)* | 726,8 | 86,4 | 62,6 | 140,4 | 6,8 | 123,3 | 116,4 |
| $C_{CO_2}$ *(%)* | 0,0 | 90,6 | 92,2 | 77,5 | 99,2 | 83,2 | 83,9 |
| $A_{CO_2}$ *(%)* | 0,0 | 88,1 | 91,4 | 80,7 | 99,1 | 83,0 | 84 |
| $SPECCA$ *(MJ/kgCO₂)* | - | 3,08 | 1,12 | -0,48 | 1,52 | 0,36 | 0,36 |
| ***Exergy*** | | | | | | | |
| $\xi$ *(%)* | 44,5 | 35,2 | 40,5 | 46,3 | 38,9 | 43,3 | 43,2 |
| $\xi'$ *(%)* | 44,5 | 40,9 | 46,1 | 50,5 | 44,6 | 48,2 | 48,1 |

Table 9 "Advanced" power plant results

| ***Power Plant Type*** | ***Benchmarks*** | | ***GSC-MAWGS*** | | | | | |
|---|---|---|---|---|---|---|---|---|
| *Concept/ KPI* | **Unabated IGCC** | **Pre-combustion $CO_2$ capture IGCC** | **Shell gasifier** | | **Pregasifier & HTW gasifier** | | **GE gasifier** | |
| | | | *Power* | *$H_2$* | *Power* | *$H_2$* | *Power* | *$H_2$* |
| ***Energy*** | | | | | | | | |
| $\eta_t$ (%) | 51,6 | 41,9 | 47,2 | -2,5 | 50,3 | 0,6 | 47,1 | -1,4 |
| $\eta_t^{H_2}$ (%) | - | - | - | 60,7 | - | 66,2 | - | 63,5 |
| $\eta_{t,eq}^{H_2}$ (%) | - | - | - | 57,9 | - | 67,0 | - | 61,8 |
| ***Environmental*** | | | | | | | | |
| $E_{CO_2}$ (kgCO₂/MWh) | 670,9 | 70,6 | 38,3 | 29,5 | 13,2 | 7,6 | 11,6 | 4,9 |
| $C_{CO_2}$ (%) | 0 | 91,5 | 94,8 | 94,8 | 98,1 | 98,5 | 98,4 | 99,1 |
| $A_{CO_2}$ (%) | 0 | 89,5 | 94,3 | - | 98,0 | - | 98,3 | - |
| $SPECCA$ (MJ/kgCO₂) | - | 2,7 | 1,03 | - | 0,28 | - | 1,02 | - |
| ***Exergy*** | | | | | | | | |
| $\xi$ (%) | 48,2 | 39,1 | 44,1 | 58,5 | 47,0 | 63,2 | 47,0 | 61,1 |
| $\xi'$ (%) | 48,2 | 44,7 | 49,9 | 69,3 | 52,8 | 70,1 | 52,8 | 71,6 |

# Appendix

The detailed description of the modelling blocks and further assumptions can be found in the Appendix section of deliverable 3.4 and in the publications shown in the section below.

# Publications

The following list of journal publications shows the scientific output from UPM in GaSTech:


1. C. Arnaiz del Pozo, S. Cloete, J.H. Cloete, Á Jiménez Álvaro and S. Amini, "The potential of chemical looping combustion using the gas switching concept to eliminate the energy penalty of $CO_2$ capture" *International Journal of Greenhouse Gas Control.* 2019, vol. 83, pp. 265-281. https://doi.org/10.1016/j.ijggc.2019.01.018.
2. C. Arnaiz del Pozo, S. Cloete, J.H Cloete, Á. Jiménez Álvaro and S. Amini, "The oxygen production pre-combustion (OPPC) IGCC plant for efficient power production with $CO_2$ capture" *Energy Conversion and Management.* 2019, vol. 201, pp. 112109. https://doi.org/10.1016/j.enconman.2019.112109
3. C. Arnaiz del Pozo, A. Jiménez Álvaro, J.H Cloete, S. Cloete and S. Amini, "Exergy Analysis of Gas Switching Chemical Looping IGCC Plants" *Energies.* 2020, vol. 13, no. 3, pp. 544. https://doi.org/10.3390/en13030544
4. C. Arnaiz del Pozo, J.H. Cloete, S. Cloete, Á Jiménez Álvaro and S. Amini, "Integration of gas switching combustion in a humid air turbine cycle for flexible power production from solid fuels with near-zero emissions of $CO_2$ and other pollutants" *International Journal of Energy Research.* 2020, https://doi.org/10.1002/er.5443
5. C. Arnaiz del Pozo, S. Cloete, P. Chiesa , Á. Jiménez Álvaro and S. Amini, "Integration of gas switching combustion and membrane reactors for exceeding 50% efficiency in flexible IGCC power plants with near-zero $CO_2$ emissions" *Energy Conversion and Management.* 2020, In press. https://doi.org/10.1016/j.ecmx.2020.100050
6. S. Szima, C. Arnaiz del Pozo, S. Cloete, S. Fogarasi, Á Jiménez Álvaro, A. Cormos, C. Cormos and S. Amini, "Techno-economic assessment of IGCC power plants using gas switching technology to minimize the energy penalty of $CO_2$ capture" *Sustainable Energy Technologies and Assessments.* Under Review.


Additionally, a 7th publication with an economic assessment of the "Advanced" plants is being carried out taking into account the $H_2$/electricity co-generation economic potential of the GSC-MAWGS IGCC concept.

The conferences and poster sessions that were attended to during the course of the project are listed below:


1. C. Arnaiz del Pozo, A. Jiménez Álvaro, J. Rodríguez Martín, S. Sánchez Orgaz, I. López Paniagua. C. González Fernández. R. Nieto Carlier. Exergy Calculation Modelling Tool for Mixtures in Power Generation: Application to WGS and ASU units of an IGCC Power Plant with Pre-combustion $CO_2$ Capture. *XI Congreso Nacional y II Internacional de Ingeniería Termodinámica*. 2019. Nº ISBN: 978-84-09-11635-5.
2. C. Arnaiz del Pozo, A. Jiménez Álvaro, J. Rodríguez Martín, S. Sánchez Orgaz, I. López Paniagua. C. González Fernández. R. Nieto Carlier. Design and Simulation of a $CO_2$

purification unit for inherent carbon capture in IGCC power plants. *XI Congreso Nacional y II Internacional de Ingeniería Termodinámica*. 2019. Nº ISBN: 978-84-09-11635-5.

3. C. Arnaiz del Pozo, A. Jiménez Álvaro, J.H. Cloete, S. Cloete, S. Amini. Integration of Gas Switching Chemical Looping Technology in IGCC plants for Inherent $CO_2$ Capture. 14th *Conference on Sustainable Development of Energy Water and Environment Systems –SDEWES*. 2019. Nº ISBN: 1847-7186.

## References

[1] T.J. Kotas, "The exergy method of thermal plant analysis", 1985.

[2] S. Cloete, M.C. Romano, P. Chiesa, G. Lozza and S. Amini, "Integration of a Gas Switching Combustion (GSC) system in integrated gasification combined cycles" *International Journal of Greenhouse Gas Control.* 2015, vol. 42, pp. 340-356.

[3] S.S. Hla, D. Park, G.J. Duffy, J.H. Edwards, D.G. Roberts, A. Ilyushechkin, L.D. Morpeth and T. Nguyen, "Kinetics of high-temperature water-gas shift reaction over two iron-based commercial catalysts using simulated coal-derived syngases" *Chem.Eng.J.* 2009, vol. 146, no. 1, pp. 148-154.

[4] E. Fernandez, J.A. Medrano, J. Melendez, M. Parco, J.L. Viviente, M. van Sint Annaland, F. Gallucci and D.A. Pacheco Tanaka, "Preparation and characterization of metallic supported thin Pd–Ag membranes for hydrogen separation" *Chemical Engineering Journal.* 2016, vol. 305, pp. 182-190.

[5] R. Anantharaman, O. Bolland, N. Booth, E. Van Dorst, E. Sanchez Fernandez, F. Franco, E. Macchi, G. Manzolini, D. Nikolic, A. Pfeffer, M. Prins, S. Rezvani and L. Robinson, "Cesar Deliverable D2.4.3. European Best Practice Guidelines For Assessment Of Co2 Capture Technologies" 2018.

[6] R. Kehlhofer, "Combined-cycle gas & steam turbine power plants", 2009.

[7] M. Gazzani, E. Macchi and G. Manzolini, "CO2 capture in integrated gasification combined cycle with SEWGS – Part A: Thermodynamic performances" *Fuel.* 2013, vol. 105, pp. 206-219.

[8] D.P. Carlos Arnaiz, Angel Jiménez Álvaro, H.C. Jan, S. Cloete and S. Amini, "Exergy Analysis of Gas Switching Chemical Looping IGCC Plants" *Energies.* 2020, vol. 13, no. 3, pp. 544.

[9] C. Arnaiz del Pozo, J.H. Cloete, S. Cloete, Á Jiménez Álvaro and S. Amini, "Integration of gas switching combustion in a humid air turbine cycle for flexible power production from solid fuels with near-zero emissions of CO2 and other pollutants" *Int.J.Energy Res.* 2020, vol. n/a.

[10] Z. Kapetaki, S. Brandani, P. Brandani and H. Ahn, "Process simulation of a dual-stage Selexol process for 95% carbon capture efficiency at an integrated gasification combined cycle power plant" *International Journal of Greenhouse Gas Control.* 2015, vol. 39, pp. 17-26.

[11] C. Arnaiz del Pozo, S. Cloete, J.H. Cloete, Á Jiménez Álvaro and S. Amini, "The potential of chemical looping combustion using the gas switching concept to eliminate the energy penalty of CO2 capture" *International Journal of Greenhouse Gas Control.* 2019, vol. 83, pp. 265-281.

[12] C. Arnaiz del Pozo, S. Cloete, J. Hendrik Cloete, Á Jiménez Álvaro and S. Amini, "The oxygen production pre-combustion (OPPC) IGCC plant for efficient power production with CO2 capture" *Energy Conversion and Management.* 2019, vol. 201, pp. 112109.

[13] C. Higman, "Gasification" 2nd ed., 2008.

[14] S. Cloete, A. Giuffrida, M. Romano, P. Chiesa, M. Pishahang and Y. Larring, "Integration of chemical looping oxygen production and chemical looping combustion in integrated gasification combined cycles" *Fuel.* 2018, vol. 220, pp. 725-743.

[15] A. Giuffrida, M. Romano and G. Lozza, "Thermodynamic Assessment of IGCC Plants with Hot Gas Desulphurization" *Applied energy.* 2010, vol. 87, no. 11, pp. 3374-3383.

[16] Arnaiz del Pozo, Carlos. Cloete, Schalk. Chiesa, Paolo, Jiménez Álvaro, Ángel. Amini, Shahriar, "Integration of gas switching combustion and membrane reactors for exceeding 50% efficiency in flexible IGCC plants with near-zero CO2 emissions" *Energy Conversion & Management.* 2020.

[17] S. Cloete, A. Tobiesen, J. Morud, M. Romano, P. Chiesa, A. Giuffrida and Y. Larring, "Economic assessment of chemical looping oxygen production and chemical looping combustion in integrated gasification combined cycles" *International Journal of Greenhouse Gas Control.* 2018, vol. 78, pp. 354-363.